Residual Analysis for Circular Cylindrical Shells under Segmental Line-Load

JAMES SHENG*
North American Aviation, Inc., Downey, Calif.
AND
JOSEPH KEMPNER†
Polytechnic Institute of Brooklyn, Brooklyn, N. Y.

In order to avoid a prohibitive amount of labor required to compute rather accurately deflections and stresses for a thin shell from usually slowly convergent infinite series, an alternative approach is suggested, namely, to stop the computations at a small number of terms and then estimate rather accurately the remainder, denoted as a "residual." In doing so, asymptotic expressions for residuals are resorted to, and the radius of convergence is complied with. This technique is applied herein to the calculation of the deflections of and stresses in a thin-walled circular cylindrical shell, simply supported at its ends and under a centrally located, uniformly distributed, inward radial line-load over a circumferential segment. For possible extension of this approach to similar boundary-value problems with loadings of axial and circumferential moments applied as distributed line-loads along the same circular segment of the cylinder, integration constants are also derived and listed.

Introduction

NOWADAYS, thin-walled shells, such as those of circular cylinders, are used extensively in almost every industry. In particular, they are widely employed as component parts of spacecraft, nuclear reactors, submarines, gas turbines, and airplanes. In most cases, the formulation of their stresses and deflections under various static or dynamic loads results in infinite series. Usually, after the first few terms, the remaining ones in the series decrease rather slowly in absolute value. As an example, the paper contributed by Bijlaard[1] on the problem of circular cylindrical shell under radial surface-load over a small rectangular area of the shell surface can be cited. As a consequence, an exceedingly large number of terms may be required to attain satisfactory accuracy in the results. Thus, the amount of work involved is prohibitive in most calculations.

To circumvent this time-consuming situation, Meck[2] suggested a reduction in the order of the differential equation when he employed the complete Donnell equation[3] for the purpose of accuracy in solving the problem of a thin cylindrical shell under a sinusoidally distributed line-load of nth harmonic in the circumferential direction. Unfortunately, the suggested order-reduction method not only defeats his original purpose but also introduces errors of extremely large magnitude, even if n is only slightly different from zero.[4]

Received by IAS August 13, 1962; revision received August 23, 1963. This paper is based on a portion of the dissertation submitted to the Polytechnic Institute of Brooklyn, June 1956, by James Sheng in partial fulfillment of the requirements for the degree of Doctor of Philosophy. The work reported was partly sponsored by the Office of Naval Research under Contract No. Nonr-839(17). The authors wish to express their thanks to F. V. Pohle for the illuminating talks with him during the course of this investigation and to the Office of Naval Research for their partial support for the work involved. The authors also wish to express their appreciation to the Space and Information Systems Division of North American Aviation Inc. and, in particular, to Francis C. Hung of the Dynamic Sciences for his help and services rendered in the preparation of this paper.

* Research Specialist, Dynamic Sciences, Space and Information Systems Division. Member AIAA.

† Professor of Applied Mechanics, Department of Aerospace Engineering and Applied Mechanics. Associate Fellow Member AIAA.

To counteract this difficulty squarely, two alternatives may be resorted to: 1) method of transform, with a hope that the infinite series originated therefrom would be more rapidly convergent; in this regard, Nash and Bridgland[5] employed the finite Fourier transform to solve Flügge's[6] equations; and 2) the technique of computing residuals,[7–10] in which a residual is defined as the remainder of the infinite series after a small number of the first few terms; this technique is used to enhance the accuracy without prohibitive labor.

In the present paper, the method of computing residuals is applied to the determination of the stresses in and deflections of a thin-walled circular cylindrical shell, simply supported at its ends and under a centrally located, uniformly distributed, inward radial line-load over a circumferential segment.

The numerical results thus obtained are designated as solution 1. The corresponding results in Refs. 8 and 11 for deflections and stresses of the same cylinder, with the exception that the uniformly distributed line-load acts along a segment in the direction of a generator of the cylinder, are designated as solution 2. Curves representing these results are shown in Figs. 1–5 for comparison.

Illustrative Example

A simply supported, thin-walled, circular cylindrical shell, under a uniformly distributed, radially inward line-load over a centrally located circumferential segment, is used as an illustrative example (see Fig. 6). If the deflections are expressed as exponentials along the generator and trigonometric functions of nth harmonics in the circumferential direction, methods based on Refs. 12 and 13 may be applied to solve Donnell's equations[14] for the deflections and stresses, caused by the action of such a localized force. For numerical calculation, the radius-thickness ratio a/h is 50, radius-length ratio a/L is $\frac{1}{5}$, the ratio $\delta/2\pi a$ comparable to δ/L in Ref. 11 for solution 2 is $\frac{1}{40}$, and Poisson's ratio ν is 0.3.

When only half of the cylindrical shell is taken into consideration, the line-load problem is transformed into one involving prescribed boundary conditions along circular boundaries. When the body force is assumed negligible, the homogeneous equilibrium equations for an element of the cylindrical shell can be employed.

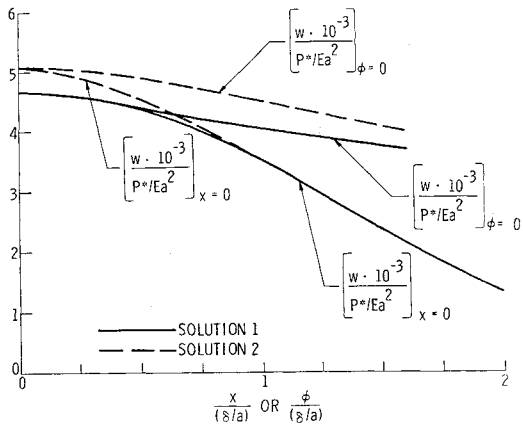

Fig. 1 Radial deflection distributions along coordinate axes due to inward radial load resultant P^* ($\delta/2\pi a = \frac{1}{40}$, $a/L = \frac{1}{5}$, $a/h = 50$).

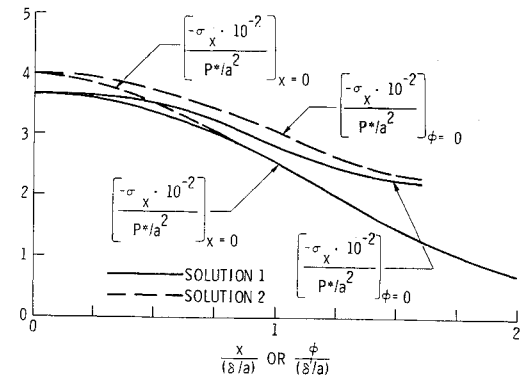

Fig. 2 Axial membrane stress distributions along coordinate axes due to inward radial load resultant P^* ($\delta/2\pi a = \frac{1}{40}$, $a/L = \frac{1}{5}$, $a/h = 50$).

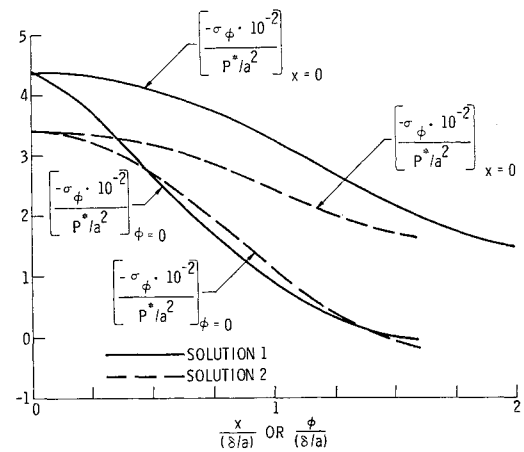

Fig. 3 Circumferential membrane stress distributions along coordinate axes due to inward radial load resultant P^* ($\delta/2\pi a = \frac{1}{40}$, $a/L = \frac{1}{5}$, $a/h = 50$).

For convenience, three nondimensional deflections, u, v, and w, and one nondimensional coordinate x may be formed by dividing the corresponding dimensional quantities by the median radius a of the cylindrical shell. With the sign convention as shown in Fig. 7, the membrane stresses (σ_x, σ_ϕ, and $\tau_{x\phi}$), the moment-resultants per unit length (M_x, M_ϕ, and $M_{x\phi}$), represented by right-hand vectors, the shear forces (Q_x and Q_ϕ), and the total effective shear forces per unit length ($Q_{x.\,\mathrm{eff}}$ and $Q_{\phi.\,\mathrm{eff}}$) can be expressed as functions of the three nondimensional deflections and their derivatives with respect to the nondimensional coordinates x and ϕ.[9, 10, 12, 13] Here ϕ denotes the circumferential angle.

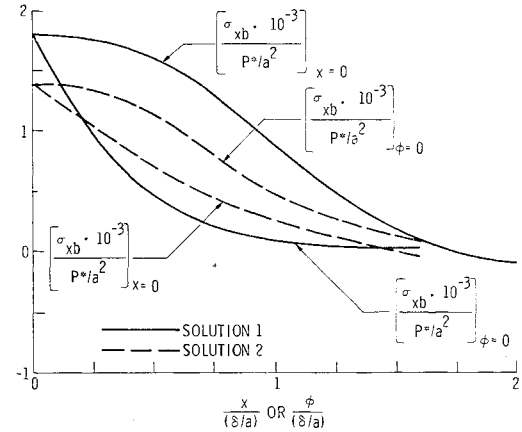

Fig. 4 Inner surface axial bending stress distributions along coordinate axes due to inward radial load resultant P^* ($\delta/2\pi a = \frac{1}{40}$, $a/L = \frac{1}{5}$, $a/h = 50$).

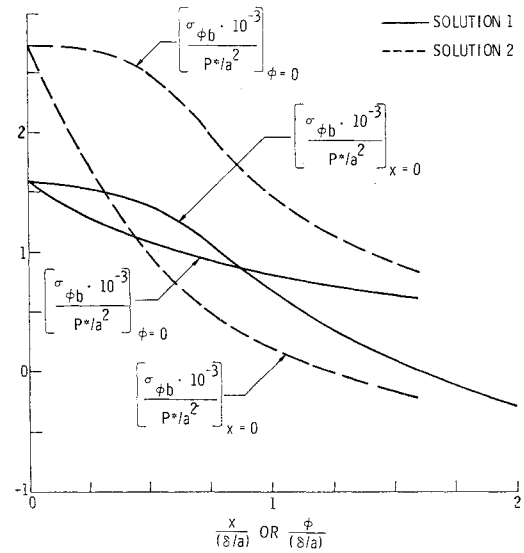

Fig. 5 Inner surface circumferential bending stress distributions along coordinate axes due to inward radial load resultant P^* ($\delta/2\pi a = \frac{1}{40}$, $a/L = \frac{1}{5}$, $a/h = 50$).

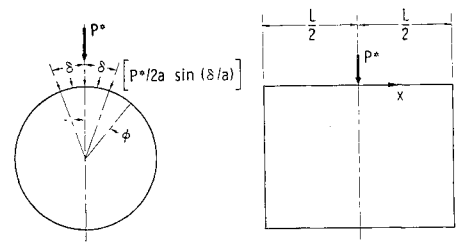

Fig. 6 Applied radial loading.

Boundary Conditions and Integration Constants

For half of the cylindrical shell (Fig. 6), the appropriate simply supported boundary conditions are $w = w_{,xx} = u_{,x} = v = 0$ at $x = L/2a$ and $w_{,x} = u = \tau_{x\phi} = 0$ and $w_{,xxx} = 1$ at $x = 0$, where the subscripts following a comma indicate partial differentiation. In the shear boundary condition $w_{,xxx}$, unity is assumed on the right-hand side of the equation for convenience. In view of the linearity of the problem, the actual value for any n can be introduced later.

The symbols for eight constants of integration $H_1, \ldots H_8$ for $n \geq 1$ and the remaining eight $G_1, \ldots G_8$ for $n = 0$, as denoted in Ref. 13, are used. When the boundary conditions are imposed,[9, 10] these constants can be evaluated as follows:

1) For $n \geq 1$,

$$\left.\begin{aligned} H_5 &= -\{n^2[n^2 - (K^2/2)] - K[n^2\alpha_2 - (K^2/2)\beta_2]\}/\{4Kn^2[(K^2/2)^2 + n^4]\} \\ H_6 &= \{n^2[n^2 + (K^2/2)] - K[n^2\beta_2 + (K^2/2)\alpha_2]\}/\{4Kn^2[(K^2/2)^2 + n^4]\} \\ H_7 &= \{n^2[n^2 - (K^2/2)] + K[n^2\alpha_1 - (K^2/2)\beta_1]\}/\{4Kn^2[(K^2/2)^2 + n^4]\} \\ H_8 &= -\{n^2[n^2 + (K^2/2)] + K[n^2\beta_1 + (K^2/2)\alpha_1]\}/\{4Kn^2[(K^2/2)^2 + n^4]\} \end{aligned}\right\} \quad (1)$$

where

$$K = [3(1 - \nu^2)]^{1/4}(a/h)^{1/2} \quad (2)$$

$$\left.\begin{aligned} \alpha_j &= \tfrac{1}{2}[\Omega - (-1)^j K + n^2/\Omega] \\ \beta_j &= \tfrac{1}{2}[\Omega + (-1)^j K - n^2/\Omega] \end{aligned}\right\} \quad (j = 1,2) \quad (3)$$

and

$$\Omega = +\{-(K^2/2) + [(K^2/2)^2 + n^4]^{1/2}\}^{1/2} \quad (4)$$

With the known constants $H_5, \ldots H_8$, the values of $H_1, \ldots H_4$ can be determined from the following relationships:

$$\left.\begin{aligned} H_{2j-1} &= H_{2j+3}S_{2j+3} + H_{2j+4}S_{2j+4} \\ H_{2j} &= H_{2j+4}S_{2j+3} - H_{2j+3}S_{2j+4} \end{aligned}\right\} \quad (j = 1,2) \quad (5)$$

where

$$\left.\begin{aligned} S_{2j+3} &= \tanh(\alpha_j L/a)/(1 + q_j) \\ S_{2j+4} &= q_j \tan(\beta_j L/a)/(1 + q_j) \end{aligned}\right\} \quad (j = 1,2) \quad (6)$$

and

$$q_j = \cos(\beta_j L/a)/\cosh(\alpha_j L/a) \quad (j = 1,2) \quad (7)$$

2) For $n = 0$,

$$\left.\begin{aligned} G_1 &= [\tanh(KL/a) - q_0 \tan(KL/a)]/[4K^3(1 + q_0)] \\ G_2 &= -[\tanh(KL/a) + q_0 \tan(KL/a)]/[4K^3(1 + q_0)] \end{aligned}\right\} \quad (8)$$

where

$$q_0 = \cos(KL/a)/\cosh(KL/a) \quad (9)$$

and

$$\left.\begin{aligned} G_3 &= G_4 = G_7 \equiv 0 \\ G_5 &= -G_6 = -1/4K^3 \\ G_8 &= \nu/4K^4 \end{aligned}\right\} \quad (10)$$

As stated before, at $x = 0$ the shear boundary condition $w_{,xxx}$ for any n is assumed to be unity for convenience. The actual value can be obtained from the Fourier expansion for the radial line-load shown in Fig. 6; P^* is the total resultant load due to the uniformly distributed radial load for the entire cylinder over an arc length of 2δ.

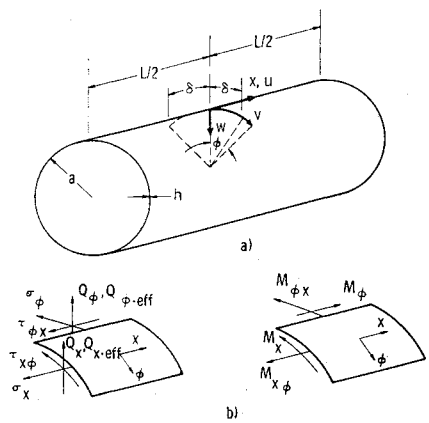

Fig. 7 Sign conventions for coordinates, deflections, membrane stresses, and internal moment and transverse shear resultants.

For half of the cylinder, from $x = 0$ to $x = +L/2a$,

$$\frac{P^*}{2} = 2\int_0^{\delta/a} qa \cos\phi d\phi$$

where q is the radial load per unit circumferential length. Therefore, the radial load per unit length for half of the cylinder is distributed such that

$$\left.\begin{aligned} q &= P^*/4a \sin(\delta/a) \quad \text{for } -\delta/a \leq \phi \leq \delta/a \\ &= 0 \quad \text{for } \delta/a < \phi < -\delta/a \end{aligned}\right\} \quad (11)$$

Up to now it has been assumed that, for any n, $w_{,xxx} = 1$ at $x = 0$, which implies

$$-Q_{x\cdot\,\text{eff}}/(D/a^2)\cos n\phi = 1 \quad (12)$$

where

$$D = Eh^3/[12(1 - \nu^2)] \quad (13)$$

is the flexural rigidity of the shell. However, if the Fourier expansion is used for the present solution, for $n = 0$,

$$-\frac{Q_{x\cdot\,\text{eff}}}{D/a^2} = \frac{P^*(\delta/a)}{4\pi(D/a)\sin(\delta/a)} \quad (14)$$

and for $n \geq 1$,

$$-\frac{Q_{x\cdot\,\text{eff}}}{(D/a^2)\cos n\phi} = \frac{P^*\sin(n\delta/a)}{2\pi(D/a)n\sin(\delta/a)} \quad (15)$$

Symbols Introduced for Conciseness

For convenience of handling and grouping terms in equations for deflections and stresses, simplifying formulas, and investigating convergence, the symbols as defined in the following are introduced:

$$\left.\begin{aligned} \bar{M}_0(x) &= [\cosh Kx \tanh(KL/a) - \sinh Kx]\cos Kx \\ \bar{N}_0(x) &= [\cosh Kx - \sinh Kx \tanh(KL/a)]\sin Kx \\ Q_0(x) &= \cosh Kx \cos Kx \tanh(KL/a) + \sinh Kx \times \sin Kx \tan(KL/a) \\ R_0(x) &= \cosh Kx \cos Kx \tan(KL/a) - \sinh Kx \sin Kx \tanh(KL/a) \end{aligned}\right\} \quad (16)$$

and

$$\left.\begin{aligned} \bar{M}_j(x) &= [\cosh\alpha_j x \tanh(\alpha_j L/a) - \sinh\alpha_j x]\cos\beta_j x \\ \bar{N}_j(x) &= [\cosh\alpha_j x - \sinh\alpha_j x \tanh(\alpha_j L/a)]\sin\beta_j x \\ Q_j(x) &= [\tanh(\alpha_j L/a) + \tanh\alpha_j x \tan\beta_j x \times \tan(\beta_j L/a)]\cosh\alpha_j x \cos\beta_j x \\ R_j(x) &= [\tan(\beta_j L/a) - \tanh\alpha_j x \tan\beta_j x \times \tanh(\alpha_j L/a)]\cosh\alpha_j x \cos\beta_j x \end{aligned}\right\} \quad (17)$$

where $j = 1$ or 2.

For further simplification in presentation of formulas, the following symbols are used:

$$T_{01}(x) = \bar{M}_0(x) - \frac{q_0 Q_0(x)}{1 + q_0} \qquad T_{02}(x) = \bar{N}_0(x) - \frac{q_0 R_0(x)}{1 + q_0} \quad (18)$$

$$\left.\begin{aligned} T_{2j+3}(x) &= \bar{M}_j(x) - \frac{q_j Q_j(x)}{1 + q_j} \\ T_{2j+4}(x) &= \bar{N}_j(x) - \frac{q_j R_j(x)}{1 + q_j} \end{aligned}\right\} \quad (j = 1,2) \quad (19)$$

Formulas for Deflections and Stresses

The maximum bending stresses at the extreme fibers are

$$\sigma_{xb} = \pm(6/h^2)M_x \qquad \sigma_{\phi b} = \pm(6/h^2)M_\phi \quad (20)$$

where the plus and minus signs, respectively, apply to points

in the wall at the inner and outer surfaces of the shell. The total stresses at these locations are obtained from the superposition of the stresses given by Eqs. (20) and their corresponding counterparts σ_x and σ_ϕ.

Use of the equations listed in Ref. 13 for w, σ_x, σ_ϕ, M_x, and M_ϕ, expressed as functions of α_j, $\beta_j (j = 1,2)$, and K, together with Eqs. (1, 5, and 10) for the integration constants, namely, $G_1, \ldots G_8$, $H_1 \ldots H_8$, and subsequent multiplication of the resulting formulas by the right-hand side of Eq. (14) for $n = 0$ and that of Eq. (15) for $n \geq 1$ before summation give the following formulas for nondimensional deflections and stresses:

$$\left(\frac{w}{P^*/Ea^2}\right)_{\substack{x\neq 0\\ \phi\neq 0}} = \frac{3(1-\nu^2)}{4K^3\pi}\left(\frac{a}{h}\right)^3 \frac{\delta/a}{\sin(\delta/a)}(T_{01}+T_{02}) + \frac{6(1-\nu^2)}{\pi\sin(\delta/a)}\left(\frac{a}{h}\right)^3 \sum_{n=1}^{\infty}\frac{\sin(n\delta/a)}{n}[(H_5T_5 - H_6T_6) + (H_7T_7 - H_8T_8)]\cos n\phi \quad (21a)$$

$$\left(-\frac{\sigma_x}{P^*/a^2}\right)_{\substack{x\neq 0\\ \phi\neq 0}} = \frac{-3(1-\nu^2)}{K^2\pi\sin(\delta/a)}\left(\frac{a}{h}\right)^3 \sum_{n=1}^{\infty} \times n\sin\left(\frac{n\delta}{a}\right)[(H_5T_6 + H_6T_5) + (H_7T_8 + H_8T_7)]\cos n\phi \quad (21b)$$

$$\left(-\frac{\sigma_\phi}{P^*/a^2}\right)_{\substack{x\neq 0\\ \phi\neq 0}} = \frac{3(1-\nu^2)}{4K^3\pi}\left(\frac{a}{h}\right)^3 \frac{\delta/a}{\sin(\delta/a)}(T_{01}+T_{02}) + \frac{3(1-\nu^2)}{K^2\pi\sin(\delta/a)}\left(\frac{a}{h}\right)^3 \sum_{n=1}^{\infty}\frac{\sin(n\delta/a)}{n} \times \{K[(K + n^2/\Omega)(H_5T_5 - H_6T_6) + (K - n^2/\Omega)(H_7T_7 = H_8T_8)] + \Omega[(K + n^2/\Omega)(H_5T_6 + H_6T_5) - (K - n^2/\Omega)(H_7T_8 + H_8T_7)]\}\cos n\phi \quad (21c)$$

$$\left(\frac{\sigma_{xb}}{P^*/a^2}\right)_{\substack{x\neq 0\\ \phi\neq 0}} = \frac{3(\delta/a)}{4K\pi\sin(\delta/a)}\left(\frac{a}{h}\right)^2 (T_{01} - T_{02}) + \frac{\nu}{2(1-\nu^2)(a/h)}\sum_{n=1}^{\infty} n^2\left(\frac{w_n}{P^*/Ea^2}\right)_{\substack{x\neq 0\\ \phi\neq 0}} - \frac{3}{\pi\sin(\delta/a)}\left(\frac{a}{h}\right)^2 \sum_{n=1}^{\infty}\frac{\sin(n\delta/a)}{n}\{\Omega[(K + n^2/\Omega)(H_5T_5 - H_6T_6) - (K - n^2/\Omega)(H_7T_7 - H_8T_8)] - K[(K + n^2/\Omega)(H_5T_6 + H_6T_5) + (K - n^2/\Omega)(H_7T_8 + H_8T_7)]\}\cos n\phi \quad (21d)$$

where w_n represents w for any $n \geq 1$.

$$\left(\frac{\sigma_{\phi b}}{P^*/a^2}\right)_{\substack{x\neq 0\\ \phi\neq 0}} = \nu\left(\frac{\sigma_{xb}}{P^*/a^2}\right)_{\substack{x\neq 0\\ \phi\neq 0}} + \frac{1}{2(a/h)}\sum_{n=1}^{\infty} n^2\left(\frac{w_n}{P^*/Ea^2}\right)_{\substack{x\neq 0\\ \phi\neq 0}} \quad (21e)$$

The grouping of terms in the formulas for deflections and stresses and the related symbols facilitates computations. These formulas are all exact ones. For special cases where $x = 0$ or $\phi = 0$ or both are equal to zero, these formulas can be considerably simplified.

Criteria for Number of Terms Required

To compute the formulas for deflections and stresses, Eqs. (3) and (4) must be used for every n for fixed x and ϕ. For satisfactory accuracy in the results, a least number of terms in each of the formulas is needed for calculation. Usually this number is quite large because the terms after the first few converge slowly in absolute value. Hence, the amount of work to meet this requirement is prohibitive in most cases. The alternative is to stop the computations at a small number of terms, beyond which replacement by the asymptotic expressions can be justified, and then estimate rather accurately the remainder, called "residual"[8-10] from these asymptotic formulas.

Table 1 Comparison of exact and approximate values for $t = \frac{1}{3}$

	Exact formula	Approximate formula	Percentage of error
Ω/n	0.946067	0.944444	0.172%
n/Ω	1.057008	1.055556	0.137%
α_1/n	1.237240	1.235702	0.124%
α_2/n	0.765835	0.764298	0.201%
$\beta_1/(K/2)$	−1.23534	−1.235702	−0.209%
$\beta_2/(K/2)$	0.764659	0.764298	0.047%

For sufficiently large n, the quantities Ω, α_j, β_j $(j = 1,2)$ may be expanded in powers of

$$t = K/(2^{1/2}n) \quad (22)$$

From Eq. (4), one can express Ω/n in terms of t; thus

$$\Omega/n = +[-t^2 + (1 + t^4)^{1/2}]^{1/2} \quad (23)$$

which may be expanded in ascending powers of t. The radius of convergence of the series in t can be established, since the zeros of the right-hand side of Eq. (23) are at $\pm (1/2^{1/2})(1 \pm i)$. The radius of convergence in each case is the absolute value of the zeros just listed. In other words,

$$0 < t < 1 \quad (24)$$

This is also true for α_j and β_j. To increase the rapidity of convergence and to make the simplification of residual formulas possible, as will be shown later, the inequality (24) is now replaced by the more stringent requirement

$$0 < t \leq \tfrac{1}{3} \quad (25)$$

Table 1 lists values obtained from exact formulas and approximate ones for comparison. The latter are derived from power series in t but are approximated by quantities involving the lowest power of t appearing therein. The small percentages of error justifies the use of the approximate formulas when $t \leq \frac{1}{3}$. The bound on t expressed in the inequality (25) is equivalent to the requirement

$$n \geq 3K/2^{1/2} \quad (26)$$

Since $K^4 = 3(1-\nu^2)(a/h)^2$, with $\nu = 0.3$, $K = 1.2854(a/h)^{1/2}$, and one gets $n \geq 2.7268(a/h)^{1/2}$. For practical calculations, the inequality $n \geq 2.75(a/h)^{1/2}$ may be used.

Now, if $\alpha_jL/a = 5$, then $\tanh(\alpha_jL/a) = 1.0000$ correct to four decimal places. Then, from Eq. (7),

$$q_j = 0.013475\cos(\beta_jL/a) \quad (27)$$

That is, if $\alpha_jL/a \geq 5$,

$$|q_j| \leq 0.013475 \quad (28)$$

which is small compared to unity.

In conclusion, the criteria for the smallest n for which the exact formulas are computed up to are all those listed below:

$$\left.\begin{array}{ll} n \geq 2.75(a/h)^{1/2} & \\ \alpha_jL/a \geq 5 & (j = 1,2) \end{array}\right\} \quad (29)$$

with the understanding that α_j approaches n as n increases indefinitely.

The criteria (29) show that n will be least for a long, thick cylinder and largest for a short, thin cylinder. To take a typical example, as considered later in this paper, $L/a = 5$ and $a/h = 50$. The least value of n is approximately 20.

Asymptotic Expressions for Residuals for $x \neq 0$

As n increases indefinitely, q_j diminishes rapidly as compared to unity, and $\bar{M}_j/\cos\beta_jx$ and $\bar{N}_j/\sin\beta_jx$ approach $e^{-\alpha_jx}$

From Eq. (23), one may obtain the power series in t for Ω and n^2/Ω as listed below:

$$\left.\begin{aligned}\Omega &= n[1 - (t^2/2) + (t^4/8) + \ldots]\\ n^2/\Omega &= n[1 + (t^2/2) + (t^4/8) - \ldots]\end{aligned}\right\} \tag{30}$$

Therefore, Ω and n^2/Ω may be assumed equal when $t^2 \ll 1$. At the same time, α_j approaches n, and β_1 and β_2 approach $(-K/2)$ and $(K/2)$, respectively, as their limits.

Then, from Eqs. (21), the residuals of the formulas for deflections and stresses can be expressed approximately in terms of the following:

$$(1/n^r)(e^{-\alpha_1 x}\cos\beta_1 x \pm e^{-\alpha_2 x}\cos\beta_2 x)$$
$$(1/n^r)(e^{-\alpha_1 x}\sin\beta_1 x \pm e^{-\alpha_2 x}\sin\beta_2 x)$$

where r is a positive integer.

But as $t^2 \ll 1$, from Eqs. (3) and (4), one finds that $(e^{-\alpha_1 x}\cos\beta_1 x - e^{-\alpha_2 x}\cos\beta_2 x)$ and $(e^{-\alpha_1 x}\sin\beta_1 x + e^{-\alpha_2 x}\sin\beta_2 x)$, respectively, are much smaller than $(e^{-\alpha_1 x}\cos\beta_1 x + e^{-\alpha_2 x}\cos\beta_2 x)$ and $(e^{-\alpha_1 x}\sin\beta_1 x - e^{-\alpha_2 x}\sin\beta_2 x)$. Therefore, only the terms

$$\left.\begin{aligned}&(1/n^r)(e^{-\alpha_1 x}\cos\beta_1 x + e^{-\alpha_2 x}\cos\beta_2 x)\\ &(1/n^r)(e^{-\alpha_1 x}\sin\beta_1 x - e^{-\alpha_2 x}\sin\beta_2 x)\end{aligned}\right\} \tag{31}$$

are retained, with r the least and next to least positive integers.

From Eqs. (21), with the aid of Eqs. (3) and (4) and the understanding that only the terms (31) are retained, one may derive the asymptotic formulas for residuals for $x \neq 0$ and $\phi \neq 0$ in the following forms:

$$\left(\frac{w_n}{P^*/Ea^2}\right)_{\substack{x\neq 0\\ \phi\neq 0}} = \frac{3(1-\nu^2)}{2\pi\sin(\delta/a)}\left(\frac{a}{h}\right)^3 \cosh\left(\frac{Kx}{2}\right) e^{-nx} \times \left[\frac{\cos(Kx/2)}{n^4} + \frac{\sin(Kx/2)}{Kn^3}\right]\left[\operatorname{sinn}\left(\frac{\delta}{a}+\phi\right) + \operatorname{sinn}\left(\frac{\delta}{a}-\phi\right)\right] \tag{32a}$$

$$\left(-\frac{(\sigma_x)_n}{P^*/a^2}\right)_{\substack{x\neq 0\\ \phi\neq 0}} = \frac{3(1-\nu^2)}{16\pi\sin(\delta/a)}\left(\frac{a}{h}\right)^3 \cosh\left(\frac{Kx}{2}\right) e^{-nx} \times \left[\frac{\cos(Kx/2)}{n^4} - 4\,\frac{\sin(Kx/2)}{K^3 n}\right] \times \left[\operatorname{sinn}\left(\frac{\delta}{a}+\phi\right) + \operatorname{sinn}\left(\frac{\delta}{a}-\phi\right)\right] \tag{32b}$$

$$\left(-\frac{(\sigma_\phi)_n}{P^*/a^2}\right)_{\substack{x\neq 0\\ \phi\neq 0}} = \frac{3(1-\nu^2)}{16\pi\sin(\delta/a)}\left(\frac{a}{h}\right)^3 \times \cosh\left(\frac{Kx}{2}\right) e^{-nx}\left[\frac{\cos(Kx/2)}{n^4} + 4\,\frac{\sin(Kx/2)}{K^3 n}\right] \times \left[\operatorname{sinn}\left(\frac{\delta}{a}+\phi\right) + \operatorname{sinn}\left(\frac{\delta}{a}-\phi\right)\right] \tag{32c}$$

$$\left(\frac{(\sigma_{xb})_n}{P^*/a^2}\right)_{\substack{x\neq 0\\ \phi\neq 0}} = \frac{3}{4\pi\sin(\delta/a)}\left(\frac{a}{h}\right)^2 \cosh\left(\frac{Kx}{2}\right) e^{-nx} \times \left[\frac{(1+\nu)\cos(Kx/2)}{n^2} - \frac{(1-\nu)\sin(Kx/2)}{Kn}\right] \times \left[\operatorname{sinn}\left(\frac{\delta}{a}+\phi\right) + \operatorname{sinn}\left(\frac{\delta}{a}-\phi\right)\right] \tag{32d}$$

$$\left(\frac{(\sigma_{\phi b})_n}{P^*/a^2}\right)_{\substack{x\neq 0\\ \phi\neq 0}} = \frac{3}{4\pi\sin(\delta/a)}\left(\frac{a}{h}\right)^2 \cosh\left(\frac{Kx}{2}\right) e^{-nx} \times \left[\frac{(1+\nu)\cos(Kx/2)}{n^2} + \frac{(1-\nu)\sin(Kx/2)}{Kn}\right] \times \left[\operatorname{sinn}\left(\frac{\delta}{a}+\phi\right) + \operatorname{sinn}\left(\frac{\delta}{a}-\phi\right)\right] \tag{32e}$$

When

$$nx \geq 3 \tag{33}$$

e^{-nx} will be $\frac{1}{20}$ at most and will diminish rapidly with increasing n. If condition (33) is satisfied, then the successive terms descend quickly enough in practice for accurate results to be obtained without the calculation of residuals.

Asymptotic Expressions for Residuals for $x = 0$

From Eqs. (32), the asymptotic expressions for residuals for $x = 0$ can be obtained in simple form. They are

$$\left.\begin{aligned}\left(\frac{w_n}{P^*/Ea^2}\right)_{\substack{x=0\\ \phi\neq 0}} &= \frac{3(1-\nu^2)}{2\pi\sin(\delta/a)}\left(\frac{a}{h}\right)^3 \times \frac{1}{n^4}\left[\operatorname{sinn}\left(\frac{\delta}{a}+\phi\right) + \operatorname{sinn}\left(\frac{\delta}{a}-\phi\right)\right]\\ \left(-\frac{(\sigma_x)_n}{P^*/a^2}\right)_{\substack{x=0\\ \phi\neq 0}} &= \left(-\frac{(\sigma\phi)_n}{P^*/a^2}\right)_{\substack{x=0\\ \phi\neq 0}} = \frac{1}{8}\left(\frac{w_n}{P^*/Ea^2}\right)_{\substack{x=0\\ \phi\neq 0}}\\ \left(\frac{(\sigma_{xb})_n}{P^*/a^2}\right)_{\substack{x=0\\ \phi\neq 0}} &= \left(\frac{(\sigma_{\phi b})_n}{P^*/a^2}\right)_{\substack{x=0\\ \phi\neq 0}} = \frac{3(1+\nu)}{4\pi\sin(\delta/a)} \times \left(\frac{a}{h}\right)^2 \frac{1}{n^2}\left[\operatorname{sinn}\left(\frac{\delta}{a}+\phi\right) + \operatorname{sinn}\left(\frac{\delta}{a}-\phi\right)\right]\end{aligned}\right\} \tag{34}$$

Numerical Evaluation of Residuals

To evaluate residuals from the asymptotic expressions for both the $x \neq 0$ and the $x = 0$ cases, Euler's method[7-10, 15] can be used. However, for the $x = 0$ case, the use of sine and cosine integrals[8-10] gives more accurate results and is considerably less time consuming. As an example, the formulation is as follows:

$$\sum_{n=N}^{\infty}\frac{1}{n^2}\sin\left[n\left(\frac{\delta}{a}+\phi\right)\right] \cong \int_N^\infty \frac{1}{z^2}\sin\left[\left(\frac{\delta}{a}+\phi\right)z\right]dz = \frac{1}{N}\sin\left[\left(\frac{\delta}{a}+\phi\right)N\right] + \left(\frac{\delta}{a}+\phi\right)\int_N^\infty \frac{1}{z}\times \cos\left[\left(\frac{\delta}{a}+\phi\right)z\right]dz \tag{35}$$

The second term under the integral sign on the right side of Eq. (35) can always be reduced to cosine integrals. Therefore, in this paper Euler's method is employed for the $x \neq 0$ case, and the cosine-integral method is used for the $x = 0$ case. In the latter, the cosine integrals are evaluated for $N = 20$.

Investigation of Convergence

To prove that the formulas for deflections and stresses under the radial load converge, one has to examine each equation. For the radial load case, one may look at the residual formulas (32) for fixed x and ϕ. Any infinite series containing terms such as e^{-nx}, $1/n^r$, where $r \geq 2$, or their products is absolutely convergent. Also, the infinite series containing terms $(1/n)\sin[n(\delta/a + \phi)]$ and $(1/n)\sin[n(\delta/a - \phi)]$, which are alternating in signs in succeeding groups of terms, are convergent. For $x = 0$, the residual formulas (34) are all absolutely convergent.

Numerical Results

Numerical results have been determined for the forementioned cylinder. For $x \neq 0$, they are evaluated at three locations of x, namely, $(1/\pi)(\delta/a)$, $(1/\pi)(3\delta/a)$, and $(1/\pi)(5\delta/a)$. Among these values of x, residuals for $x = (1/\pi)$

Table 2 Deflections and stresses along $\phi = 0$ ($a/L = \frac{1}{5}$, $a/h = 50$, $\delta/2\pi a = \frac{1}{40}$)

x	$\frac{w \times 10^{-3}}{P^*/Ea^2}$	$\frac{-\sigma_x \times 10^{-2}}{P^*/a^2}$	$\frac{-\sigma_\phi \times 10^{-2}}{P^*/a^2}$	$\frac{\sigma_{xb} \times 10^{-3}}{P^*/a^2}$	$\frac{\sigma_{\phi b} \times 10^{-3}}{P^*/a^2}$
0	4.66	3.67	4.38	1.79	1.58
$(1/\pi)(\delta/a)$	4.54	3.46	3.46	0.792	1.23
$(1/\pi)(3\delta/a)$	4.07	2.90	1.07	0.114	0.827
$(1/\pi)(5\delta/a)$	3.68	2.22	−0.0415	0.0286	0.628

Table 3 Deflections and stresses along $x = 0$ ($a/L = \frac{1}{5}$, $a/h = 50$, $\delta/2\pi a = \frac{1}{40}$)

ϕ	$\frac{w \times 10^{-3}}{P^*/Ea^2}$	$\frac{-\sigma_x \times 10^{-2}}{P^*/a^2}$	$\frac{-\sigma_\phi \times 10^{-2}}{P^*/a^2}$	$\frac{\sigma_{xb} \times 10^{-3}}{P^*/a^2}$	$\frac{\sigma_{\phi b} \times 10^{-3}}{P^*/a^2}$
0	4.66	3.67	4.38	1.79	1.58
$\delta/2a$	4.35	3.38	4.09	1.59	1.38
δ/a	3.50	2.58	3.29	0.879	0.677
$2\delta/a$	1.34	0.735	1.49	−0.0768	−0.267
$\pi/2$	−0.193	−0.401	−0.0111	−0.0105	0.0359
π	−0.189	0.0399	0.00465	−0.00905	−0.0308

(δ/a) were calculated only because the largest n used in the exact formulas is 20; as a consequence, 20 $\delta/\pi a = 1$, which is less than 3. For the other nonzero values of x, the calculation of residuals was not necessary. These may be evidenced from Eq. (33) and the related statement mentioned before.

These results are shown in Tables 2 and 3 and Figs. 1–5. Solution 1 in these figures refers to the same cylinder acted on by a uniformly distributed line-load along a segment in the generator direction[8, 11] for comparison. All the calculations are made at the locations along the generator and circumferential directions measured in units of δ/a.

Appendix

The integration constants are derived for the following two additional cases of localized loading (Figs. 8a and 8b) for possible extended use of the residual technique in the calculation of the deflections and stresses. For practical application, any localized loading on the cylindrical shell may possibly be resolved into these three cases of loading, and, because of linearity, the results from all of them can be superposed to attain the combined ones.

A. Longitudinal Moment Case

For the longitudinal moment case where a distributed line-moment is applied (Fig. 8a), the appropriate boundary conditions for half of the cylinder from $x = 0$ to $x = +L/2a$, when the cylinder is simply supported, are $w = w_{,xx} = u_{,x} = v = 0$ at $x = L/2a$ and $w = u_{,x} = v = 0$ at $x = 0$. Similarly, as in the radial load case, $w_{,xx} = 1$ at $x = 0$ is assumed for convenience. When these boundary conditions are imposed,[9, 10] the constants of integration[12] can be evaluated as follows:

1) For $n \geq 1$,

$$\left.\begin{aligned} H_1 &= -H_3 = (\Omega/4K)[(K^2/2)^2 + n^4]^{-1/2} \\ H_2 &= -H_4 = -(n^2/4K\Omega)[(K^2/2)^2 + n^4]^{-1/2} \end{aligned}\right\} \quad \text{(A1)}$$

When these constants are known, the values of $H_5, \ldots H_8$ can be determined from the following relationships:

$$\left.\begin{aligned} H_{2j+3} &= H_{2j-1}S_{2j-1} - H_{2j}S_{2j} \\ H_{2j+4} &= H_{2j-1}S_{2j} + H_{2j}S_{2j-1} \end{aligned}\right\} \quad (j = 1,2) \quad \text{(A2)}$$

where

$$\left.\begin{aligned} S_{2j-1} &= \tanh(\alpha_j L/a)/(1 - q_j) \\ S_{2j} &= q_j \tan(\beta_j L/a)/(1 - q_j) \end{aligned}\right\} \quad (j = 1,2) \quad \text{(A3)}$$

2) For $n = 0$,

$$G_1 = G_3 = G_4 = G_7 \equiv 0, \; G_2 = 1/2K^2 \quad \text{(A4)}$$

and

$$\left.\begin{aligned} G_5 &= q_0 \tan(KL/a)/2K^2(1 - q_0) \\ G_6 &= \tanh(KL/a)/2K^2(1 - q_0) \end{aligned}\right\} \quad \text{(A5)}$$

As shown in Fig. 8a, M_x^* is the total resultant moment due to the uniformly distributed longitudinal moment load for the entire cylinder over an arc length 2δ. For half the cylinder, from $x = 0$ to $x = +L/2a$,

$$\frac{M_x^*}{2} = 2\int_0^{\delta/a} qa \cos\phi d\phi$$

where q is the longitudinal moment load per unit circumferential length. Therefore, the longitudinal moment load per unit length for half the cylinder is distributed such that

$$\left.\begin{aligned} q &= M^*/4a \sin(\delta/a) \quad \text{for } -\delta/a \leq \phi \leq \delta/a \\ &= 0 \quad \text{for } \delta/a < \phi < -\delta/a \end{aligned}\right\} \quad \text{(A6)}$$

Up to now it has been assumed that, for any n, $w_{,xx} = 1$ at $x = 0$, which implies that $-M_x/(D/a)\cos n\phi = 1$. However, if the Fourier expansion is used for the present solution, for $n = 0$,

$$-M_x/(D/a) = M_x^*(\delta/a)/4\pi D \sin(\delta/a) \quad \text{(A7a)}$$

and for $n \geq 1$,

$$-M_x/(D/a)\cos n\phi = M_x^* \sin(n\delta/a)/2n\pi D \sin(\delta/a) \quad \text{(A7b)}$$

With Eqs. (A1–A5 and A7a and A7b), formulas for deflections, slopes, stresses, and their residuals may be obtained by following procedures similar to those described for the radial load case.

B. Circumferential Moment Case

For the circumferential moment case, an applied distributed radial load is considered in such a way as to be statically equivalent to a circumferential moment and a tangential force. Thus, the appropriate boundary conditions for half the cylinder from $x = 0$ to $x = +L/2a$, where the cylinder is simply supported, are essentially the same as those for the radial load case on both the boundaries. The only difference is that $\sin n\phi$ replaces $\cos n\phi$ and $-\cos n\phi$ replaces $\sin n\phi$ in the final expressions for deflections and stresses due to antisymmetric loads with respect to $\phi = 0$.

As in the radial load case, unity is assumed for $w_{,xxx}$ at $x = 0$ for convenience. The actual value can be obtained from the Fourier expansion for the circumferential moment line-load shown in Fig. 8b; M^* is the total resultant circum-

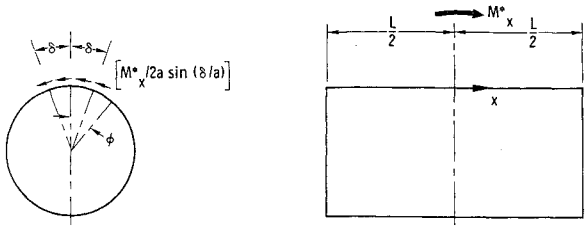

Fig. 8a Applied longitudinal moment loading.

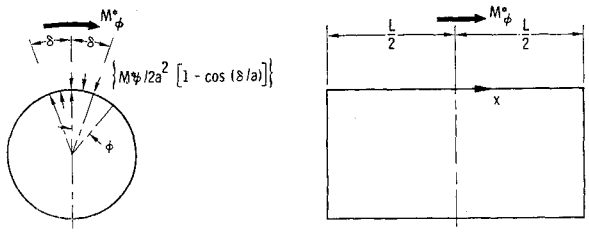

Fig. 8b Applied circumferential moment loading.

ferential moment due to the uniformly distributed antisymmetric radial load for the entire cylinder over an arc length 2δ.

For half the cylinder, from $x = 0$ to $x = +L/2a$,

$$\frac{M_\phi^*}{2} = 2\int_0^{\delta/a} qa^2 \sin\phi d\phi$$

where q is defined as in the radial load case. Consequently, the radial load per unit length for half the cylinder is distributed such that

$$\left.\begin{aligned} q &= +M_\phi^*/4a^2[1 - \cos(\delta/a)] \text{ for } 0 < \phi \leq \delta/a \\ &= -M_\phi^*/4a^2[1 - \cos(\delta/a)] \text{ for } -\delta/a \leq \phi < 0 \\ &= 0 \qquad\qquad\qquad\qquad \text{for } \delta/a < \phi < -\delta/a \end{aligned}\right\} \quad \text{(A8)}$$

Up to now it has been assumed that, for any $n \geq 1$, $w_{,xxx} = 1$ at $x = 0$, which implies

$$-Q_{x.\,\text{eff}}/(D/a^2)\sin n\phi = 1$$

However, if the Fourier expansion is used for the present solution, for $n \geq 1$,

$$-Q_{x.\,\text{eff}}/(D/a^2)\sin n\phi = [1 - \cos(n\delta/a)]M_\phi^*/2n\pi D[1 - \cos(\delta/a)] \quad \text{(A9)}$$

Using the same equations as in the radial load case with the change in trigonometric functions of n for the antisymmetric loads as mentioned previously and Eq. (A9), formulas for deflections, slopes, stresses, and their residuals may be obtained in a manner similar to the previous cases.

As noted earlier, the radial load applied is actually equivalent to the circumferential moment load M^* and a tangential load N^*, acting on the median surface of the cylindrical shell at $x = 0$ and $\phi = 0$.

For half the cylinder,

$$\frac{N^*}{2} = 2\int_0^{\delta/a} qa \sin\phi d\phi$$

or

$$N^* = 4qa[1 - \cos(\delta/a)]$$

From the first of Eqs. (A8) for q, one gets $N^* = M_\phi^*/a$. Therefore, the stresses developed due to the direct load N^* are of the order $N^*/h = M_\phi^*/ah$, which is quite small compared to the stresses due to the total circumferential moment resultant, which is of the order of $6M_\phi^*/h^2$. Therefore, the effect due to N^* can be neglected.

References

[1] Bijlaard, P. P., "Stresses from local loadings in cylindrical pressure vessels," Trans. Am. Soc. Mech. Engrs. **77**, 805–814 (1955).

[2] Meck, H. R., "Bending of a thin cylindrical shell subjected to a line load around a circumference," J. Appl. Mech. **28**, 427–433 (1961).

[3] Donnell, L. H., "A discussion of thin shell theory," *Proceedings of the Fifth International Congress of Applied Mechanics* (John Wiley and Sons Inc., New York, 1938), pp. 66–70.

[4] Sheng, J., "Discussion on Ref. 2," J. Appl. Mech. **29**, 592–594; also **29**, 766 (1962).

[5] Nash, W. A. and Bridgland, T. F., Jr., "Line loadings on finite length cylindrical shells—solution by the finite Fourier transform," Quart. J. Mech. Appl. Math. **XIV**, 129–136 (1961).

[6] Flügge, W., *Stresses in Shells* (Springer-Verlag, Berlin, 1960), pp. 218–221.

[7] Pohle, F. V., "Deformations and stresses in circular cylindrical shells caused by pipe attachments, Part III: Numerical methods," Knolls Atomic Power Lab., Schenectady, N. Y., Rept. KAPL-923 (November 1952).

[8] Kempner, J., Sheng, J., and Pohle, F. V., "Tables and curves for deformations and stresses in circular cylindrical shells under localized loadings," Polytech. Inst. Brooklyn, Brooklyn, N. Y., PIBAL Rept. 334 (October 1955).

[9] Sheng, J., "Circular cylindrical shells under circumferential line loads," Ph.D. Dissertation, Polytech. Inst. Brooklyn, Brooklyn, N. Y. (June 1956).

[10] Sheng, J. and Kempner, J., "Circular cylindrical shells under segmental circumferential line-load," Polytech. Inst. Brooklyn, Brooklyn, N. Y., PIBAL Rept. 663 (April 1963).

[11] Kempner, J., Sheng, J., and Pohle, F. V., "Tables and curves for deformations and stresses in circular cylindrical shells under localized loadings," J. Aeronaut. Sci. **24**, 119–129 (1957).

[12] Hoff, N. J., "Boundary-value problems of the thin-walled circular cylinder," J. Appl. Mech. **21**, 343–350 (1954).

[13] Pohle, F. V. and Nardo, S. V., "Simplified formulas for boundary-value problems of the thin-walled circular cylinder," J. Appl. Mech. **22**, 389–390 (1955).

[14] Donnell, L. H., "Stability of thin-walled tubes under torsion," NACA TR 479 (1933).

[15] Bromwich, T. J. I'A., *An Introduction to the Theory of Infinite Series* (Macmillan & Co., London, 1949), pp. 62–66.